

ORIGINAL ARTICLE

Myostatin signals through miR-34a to regulate *Fndc5* expression and browning of white adipocytes

X Ge¹, D Sathiakumar¹, BJJ Lua², H Kukreti², M Lee¹ and C McFarlane¹

BACKGROUND/OBJECTIVES: Myostatin (*Mstn*) has a pivotal role in glucose and lipid metabolism. *Mstn* deficiency leads to the increased browning of white adipose tissue (WAT), which results in the increased energy expenditure and protection against diet-induced obesity and insulin resistance. In this study, we investigated the molecular mechanism(s) through which *Mstn* regulates browning of white adipocytes.

METHODS: Quantitative molecular analyses were performed to assess *Mstn* regulation of miR-34a and *Fndc5* expression. miR-34a was overexpressed and repressed to investigate miR-34a regulation of *Fndc5*. Luciferase reporter analysis verified direct binding between miR-34a and the *Fndc5* 3'-untranslated region (UTR). The browning phenotype of *Mstn*^{-/-} adipocytes was assessed through the analysis of brown fat marker gene expression, mitochondrial function and infrared thermography. The role of miR-34a and *Fndc5* in this browning phenotype was verified through antibody-mediated neutralization of FNDC5, knockdown of *Fndc5* by small interfering RNA and through miR-34a gain-of-function and loss-of-function experiments.

RESULTS: *Mstn* treatment of myoblasts inhibited *Fndc5* expression, whereas the loss of *Mstn* increased *Fndc5* levels in muscles and in circulation. *Mstn* inhibition of *Fndc5* is miR-34a dependent. *Mstn* treatment of C2C12 myoblasts upregulated miR-34a expression, whereas reduced miR-34a expression was noted in *Mstn*^{-/-} muscle and WAT. Subsequent overexpression of miR-34a inhibited *Fndc5* expression, whereas blockade of miR-34a increased *Fndc5* expression in myoblasts. Reporter analysis revealed that miR-34a directly suppresses *Fndc5* expression through a miR-34a-specific binding site within the *Fndc5* 3'UTR. Importantly, *Mstn*-mediated inhibition of *Fndc5* was blocked upon miR-34a inhibition. *Mstn*^{-/-} adipocytes showed reduced miR-34a, enhanced *Fndc5* expression and increased thermogenic gene expression, which was reversed upon either neutralization of FNDC5 or *Fndc5* knockdown. In agreement, *Mstn*^{-/-} adipocytes have increased mitochondria, improved mitochondrial function and increased heat production.

CONCLUSIONS: *Mstn* regulates *Fndc5*/Irisin expression and secretion through a novel miR-34a-dependent post-transcriptional mechanism. Loss of *Mstn* in mice leads to the increased *Fndc5*/Irisin expression, which contributes to the browning of white adipocytes.

International Journal of Obesity (2017) 41, 137–148; doi:10.1038/ijo.2016.110

INTRODUCTION

The obesity epidemic represents a growing threat to health and well-being worldwide, and is one of the major risk factors for the development of cardiovascular disease, type 2 diabetes and hypertension. The recent discovery of brown adipocytes in adult humans^{1–3} has gained interest as a potential treatment for obesity. Different from white adipocytes, classic brown adipocytes show a multilocular lipid droplet phenotype and greater mitochondrial density.⁴ Although white adipocytes store energy, brown adipocytes burn energy through the production of heat by non-shivering thermogenesis, thus playing an important role in promoting total energy expenditure.^{5,6} Furthermore, brown adipocytes have a unique gene expression profile, expressing high levels of thermogenic genes such as uncoupling protein-1 (*ucp1*).⁶ In addition to brown adipose tissue (BAT), 'brown-like' adipocytes have been reported in white adipose tissue (WAT) and have been termed beige adipocytes. These beige precursor cells display a unique gene expression signature, different from both classic brown and white adipocytes.⁷ However, in response to various stimuli, beige precursor cells undergo *trans*-differentiation and adopt a 'brown-like' thermogenic gene expression profile,

with robust *ucp1* expression to promote thermogenesis.⁷ As metabolically active cells, both brown and beige adipocytes could facilitate weight loss and improve metabolic health.

Myostatin (*Mstn*), a well-studied negative regulator of skeletal muscle growth and development,^{8–10} has also been shown to inhibit fat mass accumulation¹¹ and regulate glucose homeostasis.¹² Interestingly, loss of *Mstn* in mice increases energy utilization and thus protects mice from either genetic or diet-induced obesity.^{11,13–15} Consistent with this, WAT from *Mstn*^{-/-} mice has been shown to adopt a BAT-like phenotype with associated induction of genes characteristic of brown/beige adipocytes.^{11,16} Although we know that *Mstn*^{-/-} WAT exhibits a BAT-like phenotype, and that this may explain the increased energy utilization observed in *Mstn*^{-/-} mice, the underlying molecular mechanism(s) have yet to be fully elucidated. However, our previous publication has revealed enhanced cyclooxygenase-2 (COX-2) expression in *Mstn*^{-/-} WAT.¹¹ Given the fact that elevated COX-2, and subsequent prostaglandin production/release, promotes *ucp1* expression in ingWAT,^{17,18} we hypothesized that elevated COX-2 contributes to the increased expression of *ucp1* and BAT-like phenotype in *Mstn*^{-/-} mice.¹¹ Recently, Shan *et al.*¹⁶

¹Cell & Molecular Biology Group, Singapore Institute for Clinical Sciences (A*STAR), Brenner Centre for Molecular Medicine, 30 Medical Drive, Singapore and ²School of Biological Sciences, Nanyang Technological University, Singapore. Correspondence: Dr C McFarlane, Cell & Molecular Biology Group, Singapore Institute for Clinical Sciences, Agency for Science, Technology and Research (A*STAR), 30 Medical Drive, Singapore 117609, Singapore.

E-mail: craig_mcfarlane@sics.a-star.edu.sg

Received 1 September 2015; revised 13 May 2016; accepted 17 May 2016; accepted article preview online 14 June 2016; advance online publication, 12 July 2016

revealed that inactivation of the *Mstn* gene in mice stimulates the AMP-activated protein kinase signaling, which resulted in activation of the transcriptional co-activator PPAR- γ co-activator1- α . Shan *et al.*¹⁶ further showed enhanced secretion of the PPAR- γ co-activator1- α target, Irisin, into circulation in *Mstn*^{-/-} mice, which promoted BAT-like development in *Mstn*^{-/-} WAT.

Irisin was initially described by Boström *et al.*¹⁹ and potently induces 'browning' of WAT. Irisin is derived from the extracellular N-terminal portion of the precursor protein, FNDC5 (fibronectin type III domain containing 5). Irisin targets beige precursor cells in WAT⁷ to promote the development of a BAT-like phenotype potentially through improving the PPAR- α signaling, a nuclear receptor driving *ucp1* expression. Adenovirus-mediated overexpression of Irisin in the liver protects mice from diet-induced obesity and insulin resistance.¹⁹ Irisin is substantially upregulated during endurance exercise in both mice and humans,¹⁹ as such Irisin is believed to be an important mediator that links exercise with associated health benefits. Moreover, given the role of Irisin in promoting browning of WAT, Irisin may also be a promising anti-obesity therapy.

Both *Mstn* and Irisin are myokines that are capable of modulating lipid metabolism in fat tissue and controlling whole-body energy expenditure. Evidence to date suggests that Irisin and *Mstn* function to promote and inhibit the browning of WAT, respectively; however, no work has been performed to assess whether or not these two secreted factors converge to regulate browning of WAT. Therefore, the main aim of this study was to investigate the function of *Mstn* as a regulator of the brown adipocyte-like thermogenic program in white adipocytes, and to identify a potential link between *Mstn* and Irisin during this process. In this study, we demonstrate that *Mstn* post-transcriptionally inhibits *Fndc5* expression via miR-34a in both myoblasts and adipocytes. *Mstn*^{-/-} adipocytes display increased expression of brown adipocytes-specific marker genes, suggesting that the loss of *Mstn* promotes the development of a brown adipocyte-like phenotype in a cell-autonomous manner. Consistent with the gene expression data, *Mstn*^{-/-} white adipocytes show increased mitochondria number and function, concomitant with significantly increased heat production. Our results suggest that the browning phenotype observed in *Mstn*^{-/-} adipocytes can be attributed to the decreased miR-34a expression and a subsequent increase in the expression of *Fndc5*. In summary, we propose that *Mstn* post-transcriptionally suppresses *Fndc5* expression via a miR-34-dependent mechanism in both myoblasts and white adipocytes.

MATERIALS AND METHODS

Animals

Wild-type (WT) male (C57BL/6J) mice were obtained from the Biological Resource Centre, Singapore. *Mstn*^{-/+} mice were previously gifted from

Professor Se-Jin Lee (Johns Hopkins University, Baltimore, MD, USA). Mice were maintained as previously described.¹² Experiments were conducted according to the Institutional Animal Care and Use Committee (Singapore) approved protocols.

Cell culture

Primary stromal vascular fraction (SVF) cells from inguinal WAT (ingWAT) of WT and *Mstn*^{-/-} mice (7–9 weeks old) were isolated, maintained and differentiated into mature adipocytes according to the published protocol.²⁰ Oil Red O (ORO) staining was used to detect cellular lipid accumulation in mature adipocytes, as previously published.²⁰ For neutralization of endogenous Irisin in adipocytes, SVF cells isolated from WT and *Mstn*^{-/-} mice were differentiated in the presence of either 1.25 $\mu\text{g ml}^{-1}$ anti-Fndc5 antibody (ab131390, Abcam, Cambridge, UK), which was raised against the C-terminal secreted portion of mouse FNDC5 (amino acids 50–150), or 1.25 $\mu\text{g ml}^{-1}$ rabbit IgG (X0903, Dako, Carpinteria, CA, USA) as a negative control. For recombinant *Mstn* protein treatments, WT and *Mstn*^{-/-} SVF cells were differentiated in the presence of either 4.0 $\mu\text{g ml}^{-1}$ recombinant *Mstn* protein or dialysis buffer (negative control). Expression and purification of recombinant *Mstn* protein from *Escherichia coli* were conducted according to the previously published protocol.²¹ The biological activity of the recombinant *Mstn* protein was assessed through performing a C2C12 myoblast proliferation assay.²²

Mouse C2C12 myoblasts were obtained from American Type Culture Collection (Manassas, VA, USA) and maintained or differentiated into myotubes as previously described.²³ For *Mstn* protein treatment, C2C12 myoblasts were treated with 2.5, 3.0, 3.5 and 4.0 $\mu\text{g ml}^{-1}$ recombinant *Mstn* protein for 24 h (dose-dependent treatment) or treated with 4.0 $\mu\text{g ml}^{-1}$ recombinant *Mstn* protein for 6, 12, 24 and 48 h (time-dependent treatment). Control myoblasts were treated with an equal volume of dialysis buffer.

Mouse primary myoblasts were isolated from hind-limb muscles of 4–6-week-old male WT mice (C57BL/6), using the previously described protocol.²⁴ Primary myoblasts were seeded at the density of 15 000 cells per cm^2 and then treated with either 4.0 $\mu\text{g ml}^{-1}$ recombinant *Mstn* protein or dialysis buffer for 24 h.

For all cell culture experiments, random wells were selected for treatments. The parent C2C12 myoblasts stock was tested for mycoplasma. Primary cultures were not tested for mycoplasma in this study.

Plasmids and recombinant adenovirus

The miR-34a overexpression plasmid was constructed by cloning 504 bp of murine miR-34a (mmu-miR-34a) coding region between *SpeI* and *SacI* restriction sites of the pEM157 vector (pMEV-miR-34a).

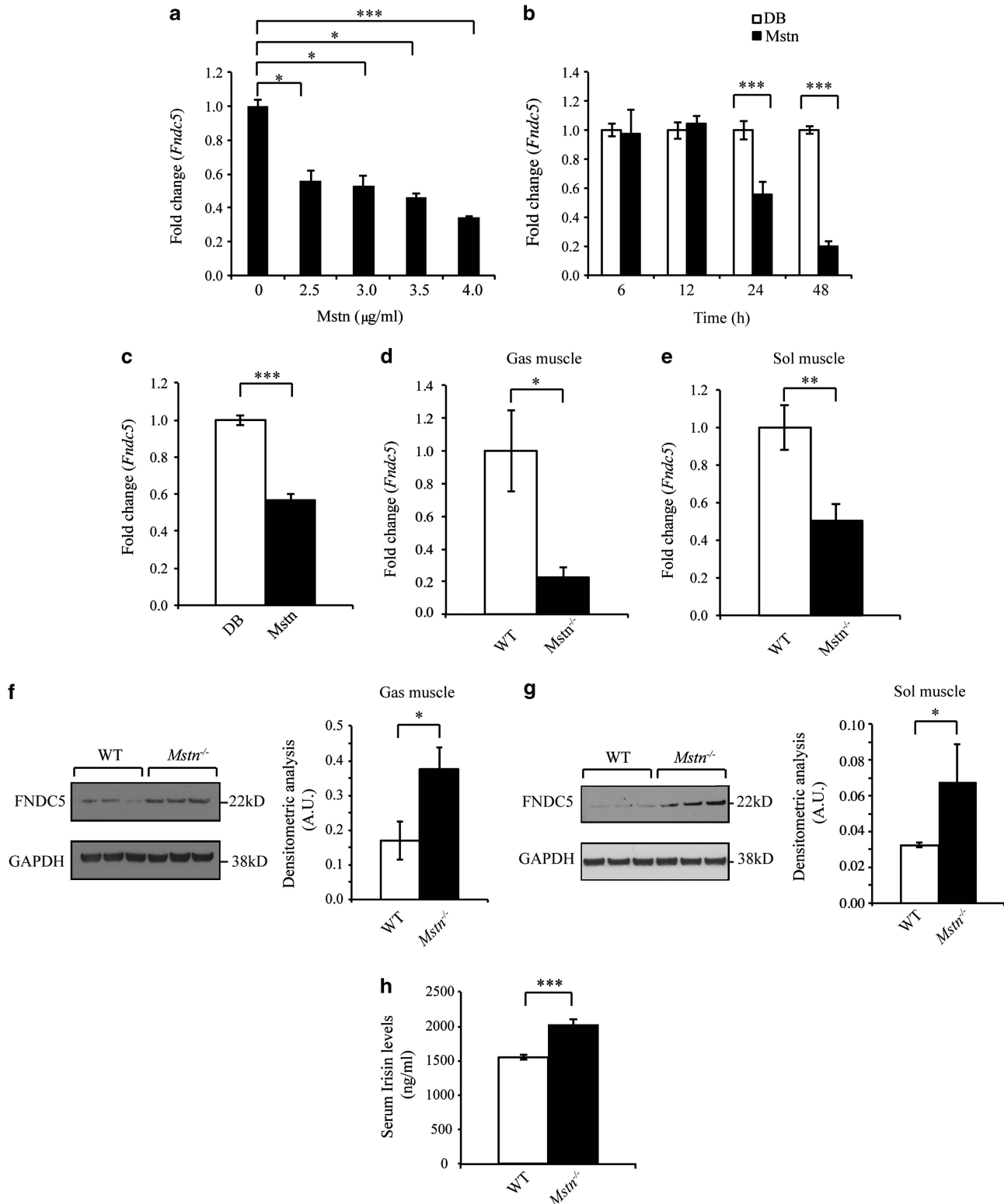
The 3'UTR region of the *Fndc5* gene (~2000 bp) was amplified by PCR and cloned into *SpeI/HindIII* sites of the pMIR-REPORT miRNA Expression Luciferase Reporter Vector (Life Technologies, Grand Island, NY, USA; pMIR-*Fndc5* 3'UTR). The putative miR-34a-binding site within the murine *Fndc5* gene 3'UTR was mutated using a megaprimer PCR-based mutagenesis approach, according to the published protocol.²⁵ The mutated *Fndc5* 3'UTR was then cloned into *SpeI/HindIII* sites of the pMIR-REPORT vector (pMIR-*Fndc5* 3'UTR-mut).

The recombinant adenovirus used to overexpress miR-34a was generated by subcloning the precursor mmu-miR-34a stem loop sequence along with 100 bp of flanking upstream and downstream sequence,

Figure 1. Myostatin is a negative regulator of *Fndc5*/Irisin expression and secretion. **(a)** *Fndc5* mRNA expression analysis (qPCR) in C2C12 myoblasts treated without (0 $\mu\text{g ml}^{-1}$) or with 2.5, 3.0, 3.5 or 4.0 $\mu\text{g ml}^{-1}$ recombinant *Mstn* protein for 24 h. Data show fold change (relative to 0 $\mu\text{g ml}^{-1}$ control) \pm s.e.m ($n=3$ biological replicates) normalized to *GAPDH* expression. * $P < 0.05$, *** $P < 0.001$. **(b)** *Fndc5* mRNA expression analysis (qPCR) in C2C12 myoblasts treated without (control, dialysis buffer) or with 4.0 $\mu\text{g ml}^{-1}$ recombinant *Mstn* protein for 6, 12, 24 or 48 h. Data show fold change (relative to respective control) \pm s.e.m ($n=3$ biological replicates) normalized to *GAPDH* expression. *** $P < 0.001$. **(c)** *Fndc5* mRNA expression analysis (qPCR) in primary myoblasts isolated from WT mice treated without (control, dialysis buffer) or with 4.0 $\mu\text{g ml}^{-1}$ recombinant *Mstn* protein for 24 h. Data show fold change (relative to control) \pm s.e.m ($n=3$ biological replicates) normalized to *GAPDH* expression. *** $P < 0.001$. *Fndc5* mRNA expression analysis (qPCR) in *M. gastrocnemius* muscle (Gas) **(d)** and *M. Soleus* muscle (Sol) **(e)** muscles from WT and *Mstn*^{-/-} mice. Data show fold change (relative to respective WT control) \pm s.e.m ($n=6$ mice per group) normalized to *GAPDH* expression. ** $P < 0.01$, *** $P < 0.001$. Immunoblot (IB) analysis of FNDC5 protein levels in Gas **(f)** and Sol **(g)** muscles from WT and *Mstn*^{-/-} mice. Graphs show densitometric analysis of FNDC5 protein levels in a.u. \pm s.e.m. ($n=3$ mice per group for Gas IB; $n=3$ WT mice vs $n=5$ *Mstn*^{-/-} mice for Sol IB) normalized to GAPDH levels. * $P < 0.05$. GAPDH levels were assessed in all IBs to ensure equal loading. Irrelevant lanes loaded adjacent to the *Mstn*^{-/-} lanes in the Gas IB have been removed. Only three representative lanes of WT and *Mstn*^{-/-} are shown in the Sol IB. **(h)** Enzyme-linked immunosorbent assay assessment of Irisin levels in serum collected from WT and *Mstn*^{-/-} mice. Data show mean \pm s.e.m. ($n=5$ mice per group). *** $P < 0.001$.

as a *Bam*HI/*Nhe*I fragment, into the pacAd5 miR-GFP/Puro Shuttle Vector (Cell Biolabs, San Diego, CA, USA), according to the manufacturer's protocols. The Shuttle Vector containing mmu-miR-34a sequence and pacAd5 9.2-100 Ad Backbone Vector were digested with *Pac*I. After purification, linearized Shuttle Vector containing the mmu-miR-34a sequence and Backbone Vector were co-transfected into 293AD cells

(catalog no.: AD-100, Cell Biolabs) using Lipofectamine 2000 reagent (Invitrogen, Carlsbad, CA, USA). Crude viral lysate was collected after 7 days incubation. Recombinant adenovirus, named pacAD5-miR-34a, was collected from crude viral lysate with three freeze/thaw cycles. Adenovirus that does not contain a miRNA fragment was used as a negative control (pacAD5-neg).



The sequences of all cloning and mutagenesis primers are provided in Supplementary Information and all the constructs were sequence verified before the use.

Transient transfection, transduction and establishment of stable cell lines

For establishment of C2C12 myoblasts stably overexpressing miR-34a, pMEV-miR-34a and control empty vector (pMEV-neg) were transfected in C2C12 myoblasts using Lipofectamine 2000 reagent (Invitrogen), according to the manufacturer's instructions. Stably overexpressing myoblasts were selected by continued neomycin (500 µg ml⁻¹) treatment for a period of 20 days until resistant colonies became visible. miR-34a-overexpressing clones were selected by quantitative PCR (qPCR) analysis of miR-34a expression. To specifically inhibit miR-34a in C2C12 myoblasts, C2C12 myoblasts were transfected with either 200 nM of AntagomiR-negative control (AntagomiR-neg) or miR-34a-specific AntagomiR (AntagomiR-34a; Sigma, Singapore) using Lipofectamine 2000 reagent (Invitrogen). After 24-h transfection, C2C12 myoblasts were treated with 4 µg ml⁻¹ recombinant Mstn protein for 24 h before RNA sample collection. For transient overexpression of miR-34a in C2C12 myotubes, 72 h differentiated C2C12 myotubes were transduced with either miR-34a-overexpressing adenovirus (pacAD5-miR-34a) or negative control adenovirus (pacAD5-neg), at multiplicities of infection of 5, 10 and 20. Twenty-four hours post transduction, medium was replaced with fresh medium and cells were allowed to grow for a further 24 h before RNA collection. For transient overexpression of miR-34a in adipocytes, *Mstn*^{-/-} SVF cells were differentiated into white adipocytes for 8 days. *Mstn*^{-/-} white adipocytes were transduced with either pacAD5-miR-34a or pacAD5-neg at multiplicities of infection of 50 for 48 h.

For transient inhibition of miR-34a in WT adipocytes, SVF cells isolated from WT ingWAT were transfected with either 200 nM of AntagomiR-neg or AntagomiR-34a (Sigma) by electroporation. Electroporation was undertaken with a Bio-Rad Gene Pulser (Hercules, CA, USA) with a capacitance of 960 µF and a voltage of 220 V. Forty-eight hours after transfection, cells were subjected to induction of white adipogenic differentiation for 8 days.

Fndc5 small interfering RNA transfection

Mstn^{-/-} SVF cells were transfected with 0.05 µM mouse *Fndc5* Accell SMARTpool small interfering RNA (siRNA) mixture (siRNA-*Fndc5*), using Accell siRNA Delivery Media, according to the manufacturer's protocol (Thermo Fisher Scientific, Waltham, MA, USA). Cells were cultured for 72 h after transfection, then lysed for qPCR. Accell SMARTpool siRNA-*Fndc5* is a pre-designed mixture of four individual *Fndc5*-targeting siRNAs, and siRNA-control is a pre-designed mixture of four individual non-targeting siRNAs. The target sequences for the siRNA-*Fndc5* and non-targeting Accell siRNA Pool (siRNA-ctrl) are provided in Supplementary Information.

Luciferase assay

miR-34a-overexpressing C2C12 myoblasts and control myoblasts were seeded onto 6-well-plates at a density of 15 000 cells per cm² and allowed to grow for 24 h before transfection. Proliferating C2C12 myoblasts were

transfected with 2 µg of pMIR-*Fndc5* 3'UTR or pMIR-*Fndc5* 3'UTR-mut reporter plasmids per well, using Lipofectamine 2000 reagent (Invitrogen), according to the manufacturer's protocol. Twenty-four hours after transfection, luciferase assay was conducted according to the previous publication.²³

RNA extraction and real-time qPCR

RNA extraction and qPCR were performed according to the previous publication.^{12,23} Ct values of the target genes were normalized against Ct values of housekeeping genes (*GAPDH* or *Hsp90ab1*) and the expression of mature miR-34a was normalized to U6. Fold change was calculated using the $\Delta\Delta\text{CT}$ method. The sequences of primers used in this study are provided in Supplementary Information.

Western blot analysis

Protein preparation and western blotting were performed according to the previous publication.¹² Proteins were prepared from homogenized muscle tissues using radioimmunoprecipitation assay buffer containing 1% IGEPAL CA-630, 0.1% SDS, 0.5% sodium deoxycholate, 50 mM NaF, 1.5 mM NaVO₄ and complete protease inhibitor (Roche, Nutley, NJ, USA). Proteins were quantified using Bradford assay reagent (Bio-Rad) and equal amounts of proteins were resolved using 4–12% gradient SDS-polyacrylamide gel electrophoresis (Invitrogen) and transferred to a nitrocellulose membrane. Deglycosylation was not performed for muscle protein extracts. Anti-FNDC5 antibody (ab181884, Abcam), which targets C-terminal of FNDC5 protein, was used to detect FNDC5 full-length protein in muscle protein extracts. Anti-GAPDH antibody (sc-32233, Santa Cruz, Biotechnology, Santa Cruz, CA, USA) was used to detect GAPDH levels as a loading control.

Irisin enzyme-linked immunosorbent assay

Circulating Irisin levels were quantified using a commercial ELISA kit (catalog no. EK-067-16; Phoenix Pharmaceuticals Inc., Burlingame, CA, USA), as per the manufacturer's protocol. Serum samples were diluted 1:100 in enzyme-linked immunosorbent assay buffer before quantification. Irisin circulation levels were calculated by nonlinear regression using GraphPad Prism 5 software (GraphPad Software, La Jolla, CA, USA).

Mitochondrial DNA per nuclear DNA ratio quantification

Relative mitochondrial DNA copy number (mtDNA) per nuclear DNA (nuDNA) ratio in WT and *Mstn*^{-/-} mature adipocytes was quantified by qPCR analysis, as described previously.²⁶ The sequence of primers used are provided in Supplementary Information. Relative fold change of mtDNA per nuDNA ratio was calculated using the $\Delta\Delta\text{CT}$ method.

Assessment of mitochondrial function

Mitochondrial function of WT and *Mstn*^{-/-} mature adipocytes was analyzed by measuring the oxygen consumption rate using an XF²⁴ Extracellular Flux Analyzer (Seahorse Bioscience, North Billerica, MA, USA), according to the manufacturer's instruction. In brief, following assessment of basal respiration rate, protein leak and ATP turnover were measured in

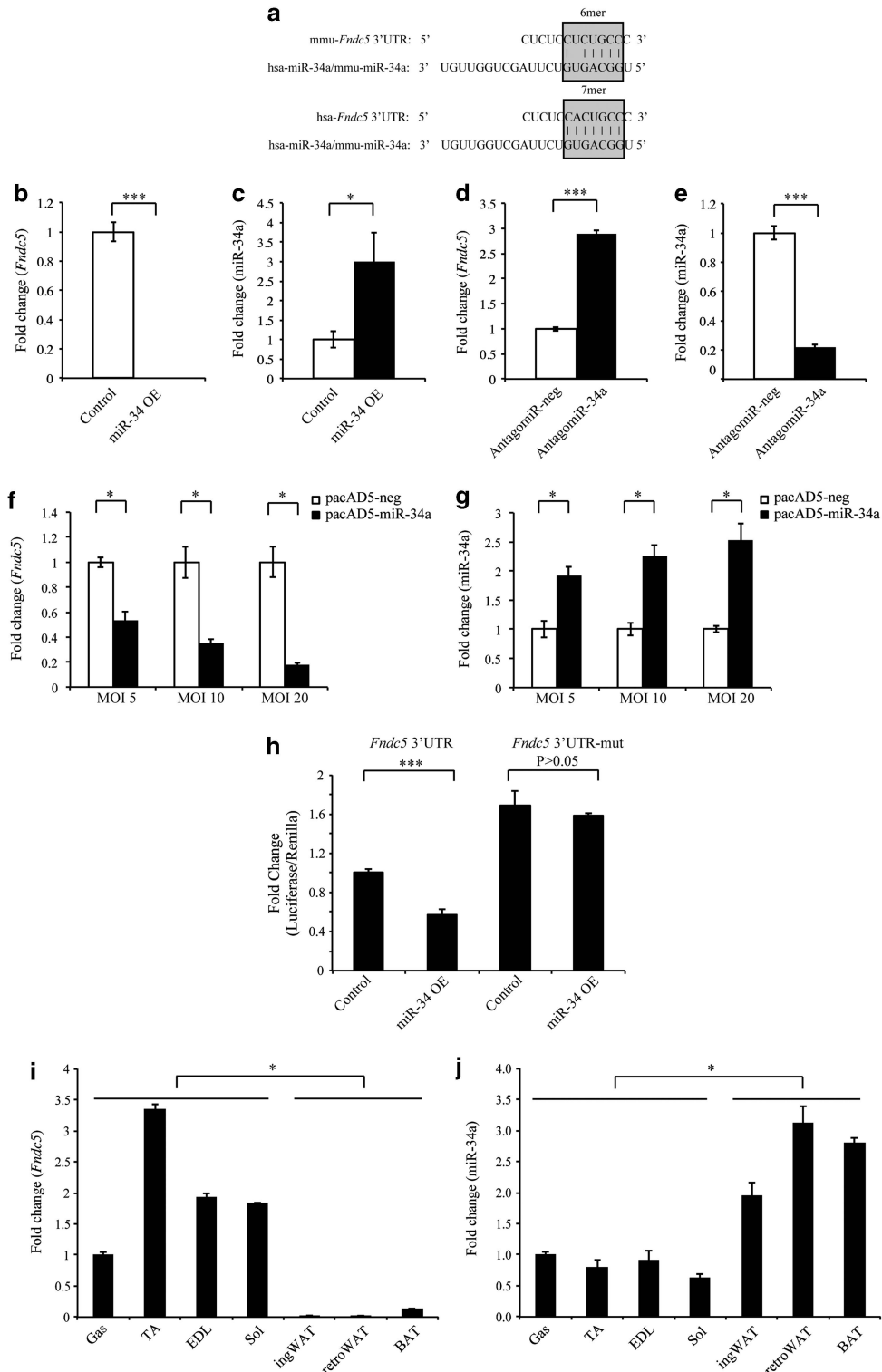
Figure 2. miR-34a targets and represses *Fndc5* expression. (a) Schematic highlighting 6mer and 7mer seed matches (gray boxes) between hsa-miR-34a (same as mmu-miR-34a) and the miR-34a-binding site in mouse (*mmu-Fndc5* 3'UTR) and human (*hsa-Fndc5* 3'UTR) *Fndc5* 3'UTR, respectively. *Fndc5* (b) and miR-34a (c) expression analysis (qPCR) in control (transfected with pMEV-neg) or miR-34a-overexpressing C2C12 myoblasts (miR-34a OE; transfected with pMEV-miR-34a). Data show fold change (relative to control) ± s.e.m (*n* = 3 biological replicates) normalized to either *GAPDH* (b) or U6 (c) expression. **P* < 0.05, ****P* < 0.001. *Fndc5* (d) and miR-34a (e) expression analysis (qPCR) in C2C12 myoblasts transfected with control (AntagomiR-neg) or miR-34a-specific AntagomiR (AntagomiR-34a). Data show fold change (relative to control) ± s.e.m (*n* = 3 biological replicates) normalized to either *GAPDH* (d) or U6 (e) expression. ****P* < 0.001. *Fndc5* (f) and miR-34a (g) expression analysis (qPCR) in 72 h differentiated C2C12 myotubes transduced with either negative control (pacAD5-neg) or miR-34a-overexpressing (pacAD5-miR-34a) adenovirus at multiplicities of infection (MOI) of 5, 10 or 20 for 24 h. Data show fold change (relative to respective controls) ± s.e.m (*n* = 3 biological replicates) normalized to either *GAPDH* (f) or U6 (g) expression. **P* < 0.05. (h) pMIR-REPORT luciferase activity analysis in C2C12 myoblasts stably overexpressing miR-34a (pMEV-miR-34a) or control empty vector (pMEV-neg), transfected with the *Fndc5* 3'UTR reporter construct (*Fndc5* 3'UTR) or the mutant *Fndc5* 3'UTR reporter construct (*Fndc5* 3'UTR-mut) with miR-34a-binding site mutated. For pMIR-REPORT transfections, data represent fold change in firefly:Renilla luciferase activity ratio, relative to control myoblasts transfected with the *Fndc5* 3'UTR reporter construct ± s.e.m (*n* = 3 biological replicates; experiment was repeated independently but data given is from one representative experiment). ****P* < 0.001. *Fndc5* (i) and miR-34a (j) expression analysis (qPCR) in *M. gastrocnemius* muscle (Gas), *M. tibialis anterior* (TA), *M. extensor digitorum longus* (EDL) muscles, *M. Soleus* muscle (Sol), inguinal white adipose tissue (ingWAT), retroperitoneal white adipose tissue (retroWAT) and brown adipose tissue (BAT) from WT mice. Data show fold change (relative to Gas) ± s.e.m (*n* = 3 mice per group) normalized to either *Hsp90ab1* (i) or U6 (j) expression. **P* < 0.05.

the presence of oligomycin (4 μ M) to inhibit ATP synthesis. Maximal mitochondrial respiratory capacity was measured by adding carbonyl cyanide-*p*-trifluoromethoxyphenylhydrazone (FCCP; 1.5 μ M). Rotenone (1 μ M) and antimycin (1 μ M) were added to assess non-mitochondrial respiration.

Infrared thermography

WT and *Mstn*^{-/-} SVF cells were seeded at the density of 10 000 cells per cm² in the center wells of 96-well-plates. Wells surrounding the plated SVF

wells contained 200 μ l phosphate-buffered saline each. Mature adipocytes were derived from SVF cells after white adipogenic differentiation, as described above. Heat production from WT and *Mstn*^{-/-} adipocytes was measured by infrared thermography. Infrared thermography was performed as previously described²⁷ with modifications. In brief, the 96-well-plates containing the cells were kept on a heating block maintained at 35 °C within an insulating box. Images were captured using an infrared camera (FLIR T420, Wilsonville, OR, USA) and then analyzed using the FLIR Tools software (FLIR). Data were collected from triplicate plates, five wells per genotype per plate.



Statistical analysis

No specific test was performed to determine the sample size. Outliers were determined using Z-scores. F-test was conducted to determine whether or not variance was equal between sample groups. One-way analysis of variance and two-tailed Student's *T*-test were used for statistical analysis. Significant levels were indicated; **P* < 0.05, ***P* < 0.01 or ****P* < 0.001. Data was expressed as mean ± s.e.m. Investigators were not blinded during allocation of experiment groups or during result analysis.

RESULTS

Mstn negatively regulates *Fndc5*/Irisin expression and secretion. Although loss of *Mstn* has been shown to increase *Fndc5* expression in skeletal muscle and primary myotubes,¹⁶ no study has to date assessed direct regulation of *Fndc5* expression by Mstn. Initially, we treated C2C12 myoblasts with recombinant Mstn protein. Subsequent qPCR analysis revealed both a dose- and time-dependent reduction in *Fndc5* expression following Mstn treatment (Figures 1a and b). Similarly, reduced *Fndc5* expression was noted in murine primary myoblasts upon Mstn treatment (Figure 1c). We next assessed *Fndc5*/Irisin expression and secretion between WT and *Mstn*^{-/-} mice. Interestingly, data suggest that although *Fndc5* messenger RNA (mRNA) expression was decreased in both fast-twitch (*Musculus gastrocnemius* muscle, Gas) and slow-twitch (*Musculus soleus* muscle, Sol) muscles from *Mstn*^{-/-} mice (Figures 1d–e), *Fndc5* protein level was significantly increased (Figures 1f–g). Consistent with this, enhanced circulating Irisin levels were also observed in *Mstn*^{-/-} mice (Figure 1h). Collectively, these data reveal that Mstn negatively regulates *Fndc5*/Irisin expression and secretion.

miR-34a targets and represses *Fndc5* expression through a miR-34a-specific binding site in the *Fndc5* 3'UTR

Analysis using the TargetScan5.1 algorithm (<http://www.targets.can.org/>) revealed one target site for microRNA-34a (miR-34a) in the 3'UTR region of both mouse and human *Fndc5* (Figure 2a). Consistent with this, *Fndc5* expression was markedly downregulated in C2C12 myoblasts stably overexpressing miR-34a (miR-34 OE; Figures 2b and c), when compared with empty vector (control)-overexpressing myoblasts, whereas specific inhibition of miR-34a through AntagomiR-34a transfection significantly increased *Fndc5* expression (Figures 2d and e). We further noted a dose-dependent decrease in *Fndc5* expression (Figure 2f) in 72 h differentiated C2C12 myotubes transduced with increasing amounts of miR-34a-overexpressing adenovirus (pacAD5-miR-34a; Figure 2g). Moreover, a significant reduction in *Fndc5* 3'UTR reporter activity was noted in miR-34a stable overexpressing myoblasts (miR-34 OE), which was reversed upon mutation of the miR-34a-binding site within the *Fndc5* 3'UTR (Figure 2h). We also observed increased *Fndc5* 3'UTR reporter activity in myoblasts transfected with *Fndc5* 3'UTR-mut, when compared with myoblasts transfected with WT *Fndc5* 3'UTR (Figure 2h). Taken together, these data suggest that miR-34a represses *Fndc5* gene expression, and that the miR-34a-binding site in the *Fndc5* 3'UTR is required.

We next assessed the role of miR-34a in regulating tissue-specific *Fndc5* expression by measuring both miR-34a and *Fndc5* expression in different tissues. *Fndc5* expression was detectable in all muscles and adipose tissues tested; however, highest *Fndc5* expression was noted in skeletal muscle (Figure 2i). This finding is in agreement with the previous studies that show Irisin is predominantly produced and secreted from skeletal muscle.^{19,28,29} Consistent with the increased *Fndc5* expression, skeletal muscles had the lowest miR-34a expression when compared with WAT and BAT (Figure 2j). These data strongly support that *Fndc5* and miR-34a expression is inversely associated

between different tissues, suggesting that miR-34a regulates *Fndc5* tissue-specific expression.

Mstn downregulates *Fndc5* expression via a miR-34a-dependent mechanism

As both Mstn and miR-34a negatively regulate *Fndc5* expression, we next investigated miR-34a involvement in Mstn regulation of *Fndc5* expression. Mature miR-34a expression was significantly increased in a dose- and time-dependent manner upon Mstn treatment (Figures 3a and b) in C2C12 myoblasts. Consistent with this, miR-34a expression was significantly reduced in both Gas muscle and ingWAT from *Mstn*^{-/-} mice (Figures 3c and d). Importantly, AntagomiR-mediated inhibition of miR-34a (AntagomiR-34a) in C2C12 myoblasts led to increased expression of *Fndc5* over and above endogenous levels and also prevented Mstn-mediated inhibition of *Fndc5* (Figure 3e). Taken together, these data suggest that Mstn inhibition of *Fndc5* is miR-34a dependent.

Loss of *Mstn* drives browning of white adipocytes *in vitro* through miR-34a regulation of *Fndc5* expression

As we observed reduced expression of miR-34a in ingWAT isolated from *Mstn*^{-/-} mice (Figure 3d), we next assessed the expression of *Fndc5* and miR-34a in differentiated white adipocytes derived from WT and *Mstn*^{-/-} SVF cells. Although Oil Red O staining revealed similar lipid accumulation during adipogenic differentiation between adipocytes derived from WT and *Mstn*^{-/-} SVF cells (Figure 4a); significantly reduced miR-34a expression, concomitant with the increased *Fndc5* expression, was observed in *Mstn*^{-/-} mature white adipocytes (Figures 4b and c). Consistent with this, significantly increased expression of several BAT marker genes, including *ucp1*, *cox7a1*, *ebf3*, *hsp7* and *cidea*, was noted in *Mstn*^{-/-} mature white adipocytes, when compared with WT adipocytes (Figure 4d). Conversely, the expression of genes characteristic of white adipocytes, such as *lep* (*leptin*) and *adipoq* (*adiponectin*), was repressed in *Mstn*^{-/-} mature white adipocytes (Figure 4d). These data suggest that the loss of *Mstn* in mature adipocytes leads to the reduced miR-34a expression, increased expression of *Fndc5* and activation of brown adipocyte-specific marker genes.

As *Mstn*^{-/-} mature white adipocytes displayed increased brown adipocyte gene expression, we further investigated the effects of *Mstn* inactivation in mature adipocytes on mitochondrial number and function. We observed an increase in the mtDNA copy number to nuDNA copy number (mtDNA:nuDNA) ratio in *Mstn*^{-/-} mature white adipocytes (Figure 4e). Analysis of adipocyte bioenergetic profiles using an XF^e24 extracellular flux analyzer (Seahorse Bioscience) demonstrated that basal mitochondrial respiration, OCR due to proton leak and maximal mitochondrial respiratory capacity were increased in *Mstn*^{-/-} mature adipocytes (Figure 4f). Consistent with the increased thermogenic gene expression, infrared thermography revealed a significant increase in heat production in *Mstn*^{-/-} mature adipocytes, which suggests enhanced thermogenic capacity (Figure 4g). Taken together, these data indicate that the loss of *Mstn* promotes induction of a 'browning' program in mature white adipocytes, which was evidenced through upregulation of brown adipocytes-specific genes, increased mitochondria number, improved mitochondrial activity and greater thermogenic capacity.

Next, we assessed whether or not the browning phenotype noted in *Mstn*^{-/-} mature adipocytes was due to the increased expression of *Fndc5*/Irisin. As such, we neutralized Irisin in the culture medium of *Mstn*^{-/-} and WT SVF cells during *in vitro* adipogenic differentiation using an *Fndc5*-specific antibody and assessed lipid droplet accumulation through Oil Red O staining and the expression of BAT and WAT marker genes in SVF-derived mature adipocytes. No significant difference in lipid accumulation

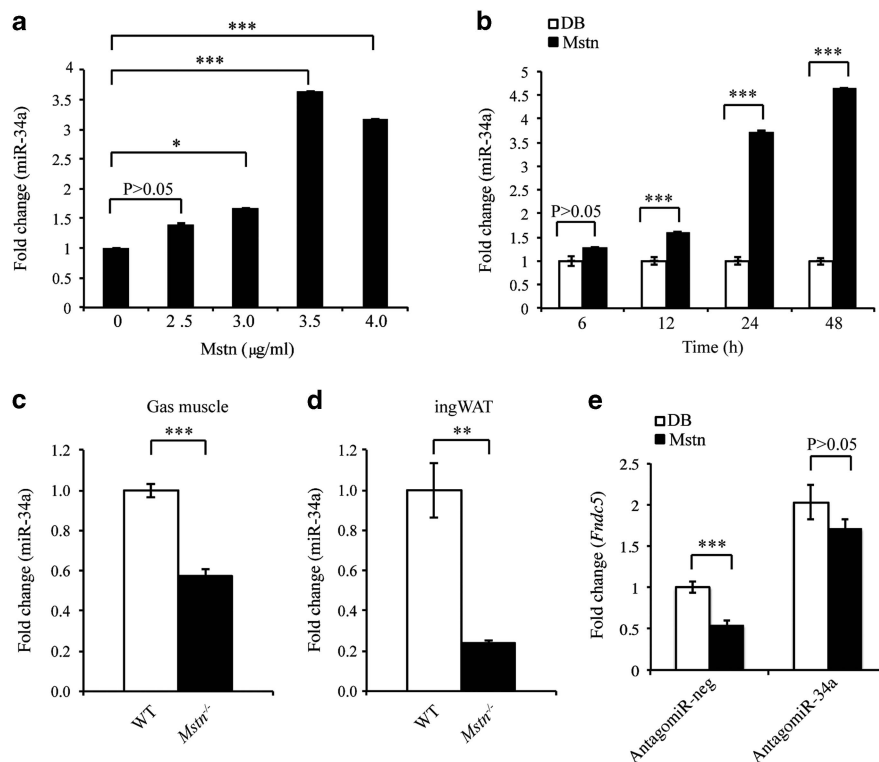


Figure 3. Mstn inhibits *Fndc5* gene expression via a miR-34a-dependent mechanism. **(a)** Mature miR-34a expression analysis (qPCR) in C2C12 myoblasts treated without ($0 \mu\text{g ml}^{-1}$) or with 2.5, 3.0, 3.5 or $4.0 \mu\text{g ml}^{-1}$ recombinant Mstn protein for 24 h. Data show fold change (relative to $0 \mu\text{g ml}^{-1}$ control) \pm s.e.m ($n=3$ biological replicates) normalized to U6 expression. $*P < 0.05$, $***P < 0.001$. **(b)** Mature miR-34a expression analysis (qPCR) in C2C12 myoblasts treated without (control, dialysis buffer) or with $4.0 \mu\text{g ml}^{-1}$ recombinant Mstn protein for 6, 12, 24 or 48 h. Data show fold change (relative to respective Control) \pm s.e.m ($n=3$ biological replicates) normalized to U6 expression. $***P < 0.001$. Mature miR-34a expression analysis (qPCR) in Gas muscle **(c)** and ingWAT **(d)** collected from WT and *Mstn*^{-/-} mice. Data show fold change (relative to WT Control) \pm s.e.m ($n=5$ mice per group) normalized to U6 expression. $**P < 0.01$, $***P < 0.001$. **(e)** *Fndc5* mRNA expression analysis (qPCR) in C2C12 myoblasts transfected with either negative control AntagomiR (AntagomiR-neg) or miR-34a-specific AntagomiR (AntagomiR-34a) for 24 h, followed by a further 24 h in the absence (control, dialysis buffer) or presence of $4.0 \mu\text{g ml}^{-1}$ recombinant Mstn protein (Mstn). Data show fold change (relative to AntagomiR-neg) \pm s.e.m ($n=3$ biological replicates) normalized to *GAPDH* expression. $***P < 0.001$.

was noted between WT and *Mstn*^{-/-} mature adipocytes treated with either control IgG or anti-*Fndc5*-specific antibody (Figure 5a). However, a significant reduction in expression of BAT marker genes (*ucp1*, *cox7a1*, *ebf3*, *hsph7* and *cidea*) and increased expression of WAT marker genes (*lep* and *ap2*) were observed in *Mstn*^{-/-} mature adipocytes upon antibody-mediated neutralization of *Fndc5* (Figure 5b). We further knocked down endogenous *Fndc5* expression (Figure 5c) in *Mstn*^{-/-} SVF cells by transfecting cells with small interfering RNA (siRNA) targeting mouse *Fndc5* mRNA (siRNA-*Fndc5*). Subsequent analysis revealed reduced *ucp1* expression in siRNA-*Fndc5*-transfected SVF cells, compared with SVF cells transfected with control non-targeting siRNA (siRNA-ctrl; Figure 5d). These data reveal that *Fndc5*/Irisin contributes, at least in part, to the increased expression of *ucp1* observed in *Mstn*^{-/-} adipocytes/SVF cells.

Given the above results, we hypothesized that Mstn represses *Fndc5* expression via miR-34a in adipocytes. Consistent with this hypothesis, Mstn treatment of WT SVF cells during *in vitro* adipogenic differentiation resulted in a significantly increased miR-34a expression (Figure 5e), concomitant with the reduced *Fndc5* expression (Figure 5f), which was also associated with the decreased expression of several WAT (*lep* and *adipoq*) and BAT marker genes (*ucp1*, *cox7a1* and *cidea*; Figure 5g). A similar decrease in *ucp1*, *cox7a1* and *cidea* was noted in Mstn-treated *Mstn*^{-/-} SVF cells during *in vitro* adipogenic differentiation. However, increased expression of the BAT marker genes, *ebf3* and *hsph7*, was noted upon Mstn treatment in WT mature

adipocytes. In addition, inhibition of miR-34a expression in WT mature adipocytes by AntagomiR-34a (Figure 5h) led to enhanced *Fndc5* (Figure 5i) and *ucp1* expression (Figure 5j). Furthermore, adenoviral-mediated overexpression of miR-34a in *Mstn*^{-/-} mature adipocytes (Figure 5k) led to the decreased *Fndc5* (Figure 5l) and *ucp1* expression (Figure 5m). These results indicate that Mstn has a role in the browning of white adipocytes through regulating endogenous *Fndc5* expression through a miR-34a-dependent mechanism.

DISCUSSION

Our previously published results revealed that the loss of *Mstn* in mice increases total energy expenditure and protects against high-fat diet-induced obesity and insulin resistance.¹¹ Although we know that enhanced browning of WAT in *Mstn*^{-/-} mice was, at least in part, responsible for the increased energy expenditure and resistance to high-fat diet-induced obesity observed, the underlying molecular mechanism(s) behind this phenomenon remained to be fully understood. In 2012, Irisin was discovered as a key exercise-induced myokine that promotes browning of WAT and increased energy expenditure.¹⁹ Recently, Shan *et al.*¹⁶ revealed that the loss of *Mstn* promotes increased *Fndc5*/Irisin expression, through the activating AMP-activated protein kinase–PPAR- γ co-activator1- α signaling, suggesting that the browning phenotype observed in *Mstn*^{-/-} mice may be due to elevated Irisin. We have now described a novel miR-34a-dependent post-transcriptional

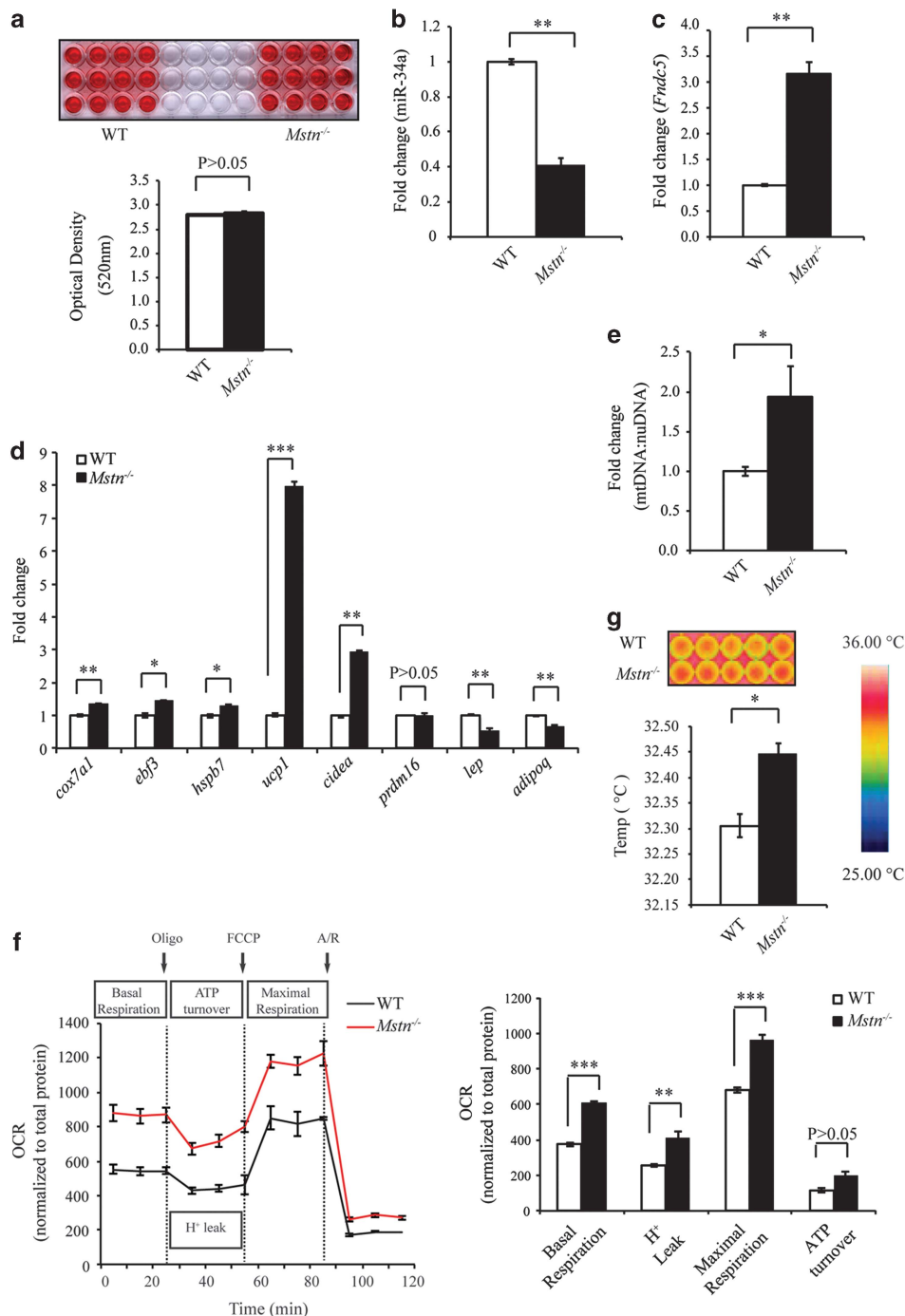


Figure 4. Loss of *Mstn* promotes the browning of white adipocytes. **(a)** Oil Red O (ORO) staining of stromal vascular fraction (SVF)-derived adipocytes from WT and *Mstn*^{-/-} mice. Graph displays quantification of ORO staining (OD 520 nm). miR-34a **(b)** and *Fndc5* **(c)** expression analysis (qPCR) in WT and *Mstn*^{-/-} adipocytes. Data show fold change (relative to respective WT control) ± s.e.m (*n* = 3 biological replicates; experiment was repeated independently, but the data given are from one representative experiment) normalized to U6 **(b)** or *GAPDH* **(c)** expression. ***P* < 0.01. **(d)** BAT (*cox7a1*, *ebf3*, *hspb7*, *ucp1*, *cidea* and *prdm16*) and WAT (*lep* and *adipoq*) marker gene expression analysis (qPCR) in WT and *Mstn*^{-/-} adipocytes. Data show fold change (relative to respective WT control) ± s.e.m (*n* = 3 biological replicates; experiment was repeated independently, but the data given are from one representative experiment) normalized to *GAPDH* expression. **P* < 0.05, ***P* < 0.01, ****P* < 0.001. **(e)** mtDNA:nuDNA ratio (qPCR) in WT and *Mstn*^{-/-} white adipocytes. Data show fold change (relative to respective WT control) ± s.e.m (*n* = 3 biological replicates). **P* < 0.05. **(f)** Left: oxygen consumption rate (OCR) measured by XF²⁴ extracellular flux analyzer (Seahorse Bioscience) in WT and *Mstn*^{-/-} adipocytes at basal and after sequential injection of oligomycin (Oligo), cyanide-*p*-trifluoromethoxyphenylhydrazone (FCCP) and antimycin+rotenone (A/R). Right: graph showing basal OCR, OCR resulting from proton leak (H⁺ leak), ATP-linked OCR and maximal OCR in adipocytes from WT and *Mstn*^{-/-} mice. Data show OCR normalized against total protein concentration ± s.e.m (*n* = 4 biological replicates; experiment was repeated independently, but the data given are from one representative experiment). ***P* < 0.01, ****P* < 0.001. **(g)** Infrared thermographic images of WT and *Mstn*^{-/-} adipocytes. Color representation of the temperature scale is given. Graph displays quantification of heat production in WT and *Mstn*^{-/-} adipocytes. Data show mean temperature ± s.e.m (*n* = 3 biological replicates; experiment was repeated independently, but the data given are from one representative experiment). **P* < 0.05.

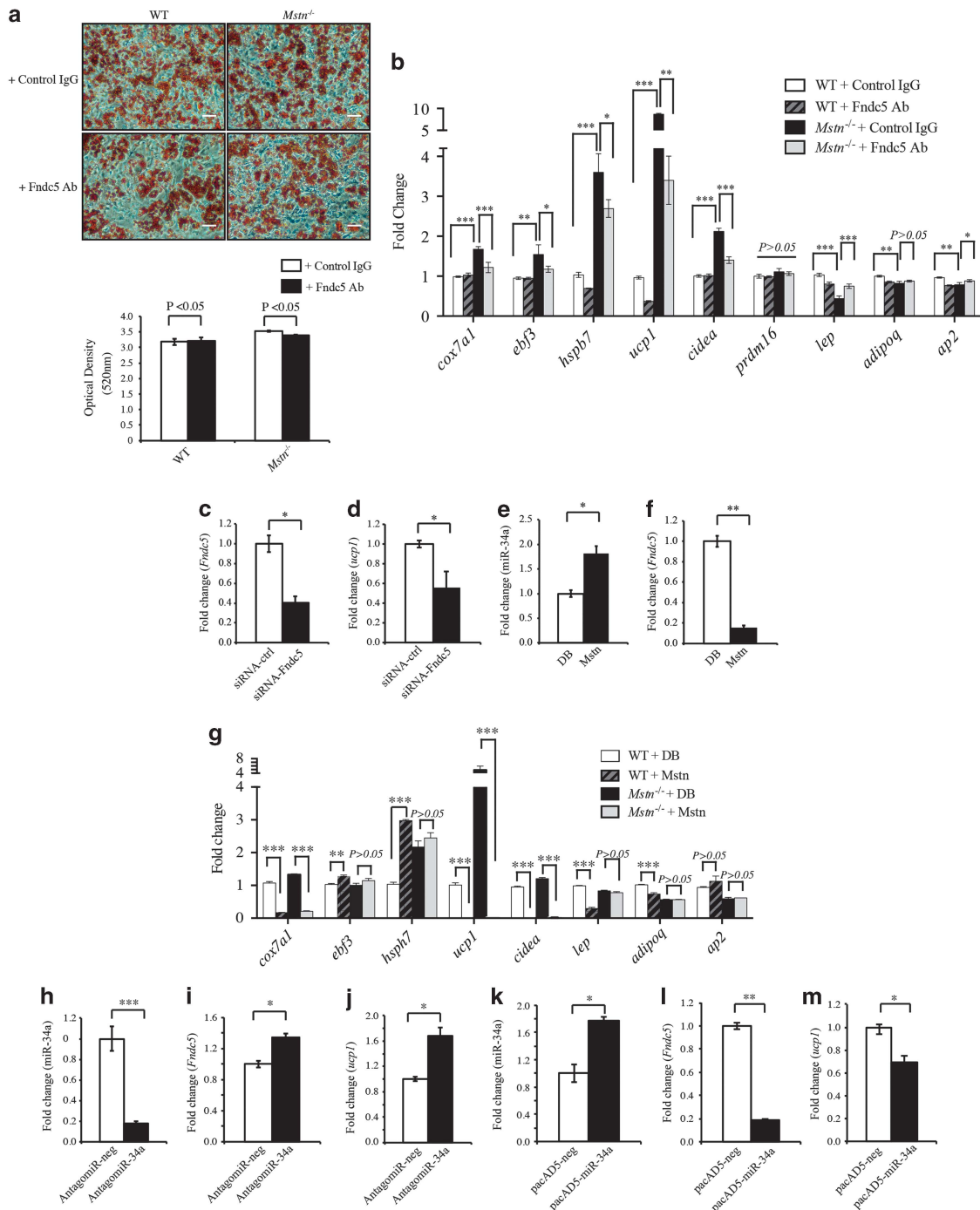


Figure 5. Mstn regulation of *Fndc5* expression and browning in white adipocytes is miR-34a dependent. **(a)** Representative images of Oil Red O (ORO) staining of WT and *Mstn*^{-/-} mature adipocytes treated with either rabbit IgG (control IgG) or with anti-Fndc5-specific antibody (Fndc5 Ab). Scale bar = 100 μm. Graph displays quantification of ORO staining (OD 520 nm). **(b)** BAT (*cox7a1*, *ebf3*, *hspb7*, *ucp1*, *cidea* and *prdm16*) and WAT (*lep*, *adipoq* and *ap2*) marker gene expression analysis (qPCR) in WT and *Mstn*^{-/-} adipocytes treated with rabbit IgG (control) or with Fndc5-neutralizing antibody (Fndc5 Ab). Data show fold change (relative to control) ± s.e.m (*n* = 3 biological replicates; experiment was repeated independently, but the data given are from one representative experiment) normalized to *GAPDH* expression. **P* < 0.05, ***P* < 0.01. *Fndc5* **(c)** and *ucp1* **(d)** mRNA expression analysis (qPCR) in *Mstn*^{-/-} SVF cells transfected with either 0.05 μM of *Fndc5*-specific siRNA pool (siRNA-Fndc5) or with 0.05 μM of non-targeting siRNA pool (siRNA-ctrl) for 72 h. Data show fold change (relative to respective control) ± s.e.m (*n* = 3 biological replicates) normalized to *GAPDH* expression. **P* < 0.05. miR-34a **(e)**, *Fndc5* **(f)**, BAT (*cox7a1*, *ebf3*, *hspb7*, *ucp1*, *cidea* and *prdm16*) and WAT (*lep*, *adipoq* and *ap2*) **(g)** marker gene expression analysis (qPCR) in WT and/or *Mstn*^{-/-} adipocytes treated without (control, dialysis buffer) or with 4.0 μg ml⁻¹ recombinant Mstn protein (Mstn). Data show fold change (relative to respective control) ± s.e.m (*n* = 3 biological replicates) normalized to U6 **(e)** or *GAPDH* **(f, g)** expression. **P* < 0.05, ****P* < 0.01. Mature miR-34a **(h)**, *Fndc5* **(i)** and *ucp1* **(j)** expression analysis (qPCR) in differentiated white adipocytes from WT SVF cells transfected with either negative control AntagomiR (AntagomiR-neg) or miR-34a-specific AntagomiR (AntagomiR-34a). Data show fold change (relative to AntagomiR-neg) ± s.e.m (*n* = 3 biological replicates) normalized to U6 **(h)** or *GAPDH* **(i, j)** expression. **P* < 0.05, ****P* < 0.001. Mature miR-34a **(k)**, *Fndc5* **(l)** and *ucp1* **(m)** expression analysis (qPCR) in *Mstn*^{-/-} differentiated SVF-derived white adipocytes after transduction with either negative control adenovirus (pacAD5-neg) or miR-34a-overexpressing adenovirus (pacAD5-miR-34a) at multiplicities of infection (MOI) of 50 for 48 h. Data show fold change (relative to pacAD5-neg) ± s.e.m (*n* = 3 biological replicates) normalized to either U6 **(k)** or *GAPDH* **(l and m)** expression. **P* < 0.05, ***P* < 0.01.

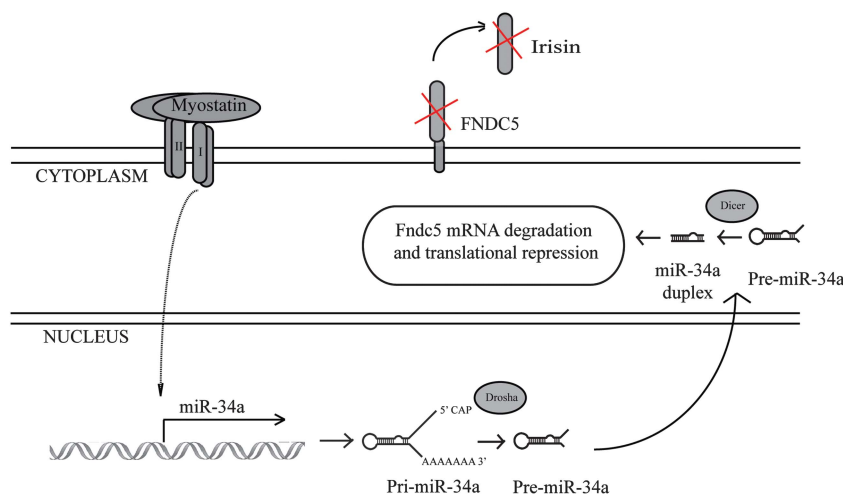


Figure 6. Mstn modulates post-transcriptional expression of *Fndc5* via a miR-34a-dependent mechanism. Elevated Mstn levels results in interaction of Mstn with its cell surface receptors and subsequent activation of Mstn downstream signaling. Activated Mstn signaling promotes increased expression of miR-34a, which subsequently targets and inhibits *Fndc5* mRNA. We propose that the loss of *Mstn* signaling results in both decreased miR-34a expression and enhanced *Fndc5* expression and Irisin secretion, contributing at least in part to the pronounced browning phenotype observed in *Mstn*^{-/-} WAT.

mechanism through which Mstn regulates *Fndc5*/Irisin and thus browning of white adipocytes. Moreover, we now show that the absence of *Mstn* promotes browning of white adipocytes through autocrine regulation of endogenous *Fndc5*/Irisin expression in white adipocytes. Interestingly, in contrast to results presented by Shan *et al.*,¹⁶ we find the decreased *Fndc5* mRNA expression, together with the increased *Fndc5* protein level in skeletal muscles of *Mstn*^{-/-} mice (Figures 1d–g). This result suggests the existence of a potential negative autoregulatory feedback loop, where the elevated *Fndc5*/Irisin protein levels found in muscle and in circulation, in turn inhibits *Fndc5* expression. However, as we observed the increased *Fndc5* mRNA expression in ingWAT of *Mstn*^{-/-} mice, compared with WAT from WT mice (data not shown), this negative autoregulatory mechanism may be skeletal muscle tissue specific. However, further work will need to be undertaken to verify the existence of an Irisin negative autoregulatory feedback loop and the potential role that this has in regulation of Irisin function.

Although we have shown that Mstn upregulates miR-34a, the molecular mechanism(s) behind this regulation remains to be elucidated. However, unpublished data from our lab suggests that Mstn may transcriptionally regulate miR-34a expression, as we observed the increased expression of both precursor and mature miR-34a upon exogenous Mstn treatment in C2C12 myoblasts (data not shown). Nonetheless, we cannot rule out the possibility that Mstn may also regulate miR-34a processing; as such further work is required to clarify this.

It is important to highlight that the above data were generated using mice and murine cell culture model systems. As such, further work should be undertaken to investigate the role of Mstn and miR-34a in regulating *Fndc5* expression in humans. This is underscored by the findings of a recent publication that confirmed, through mass spectrometry, the existence of full-length circulating Irisin protein in humans.³⁰ Both Mstn and Irisin proteins are remarkably well conserved across species, with 100% identical amino-acid sequence of mature Mstn and Irisin proteins between mouse and human.^{19,31} Together with the fact that human and mouse miR-34a sequences are identical (Figure 2a), it is quite possible that the same regulatory mechanism outlined here exists in humans. Consistent with this, higher Mstn secretion has been observed in obese patients,³² whereas the decreased Mstn expression was noted in skeletal muscle after weight loss

due to biliopancreatic diversion.³³ In addition, higher expression of miR-34a was found in adipocytes from obese individuals³⁴ and in the liver of type 2 diabetes patients.³³ In addition, research also suggests that Irisin levels are significantly reduced in obese^{35,36} and type 2 diabetes patients.^{37–39} Taken together, these correlative data suggest that Mstn may also regulate *Fndc5* expression in humans through miR-34a; however, further work will need to be performed to validate this.

Recent published evidence suggests a role for miR-34a in regulating browning of WAT.^{40,41} Fu *et al.* has revealed that miR-34a inhibits the browning transcriptional program in all types of WAT through interfering with fibroblast growth factor 21 (FGF21) signaling.^{40,41} Inhibition of miR-34a in adipose tissues or adipocytes improved FGF21 sensitivity, whereas overexpression of miR-34a reversed cold-exposure-induced browning phenotype in 3T3-L1 adipocytes.⁴⁰ FGF21 robustly induces a BAT-like phenotype in WAT through the activating PPAR-γ co-activator1-α-UCP1 signaling⁴² and is considered as a potential target for the treatment of obesity-related diseases such as diabetes.⁴³ Similar to FGF21, Irisin is another potent ‘browning agent’¹⁹ and as we have shown here the Irisin precursor gene *Fndc5* is also targeted by miR-34a. These data suggest that miR-34a is a general inhibitor of WAT browning, through interfering with the signaling of at least two key regulators of browning, FGF21 and Irisin. Future studies using miR-34a gain-of-function or loss-of-function mouse models will help us to further clarify the role of miR-34a in regulating Irisin level, as well as the impact of this regulation on systemic glucose and lipid metabolism in multiple tissues.

In contrast to the study by Shan *et al.*,¹⁶ we find a substantial difference between WT and *Mstn*^{-/-} adipocytes with respect to gene expression and function. Compared with WT adipocytes, we observed that *Mstn*^{-/-} adipocytes display upregulated thermogenic gene expression (Figure 4d), greater mitochondria number (Figure 4e), enhanced mitochondrial function (Figure 4f) and a significant, albeit modest, increase in heat production (Figure 4g). Therefore, contrary to the results presented by Shan *et al.*, we hypothesize that the loss of *Mstn* in white adipocytes results in cell-autonomous browning due to both reduced miR-34a expression (Figure 4b) and increased *Fndc5* expression (Figure 4c) in *Mstn*^{-/-} adipocytes. In agreement with this, Roca-Rivada *et al.*²⁹ have previously demonstrated that WAT expresses and secretes *Fndc5*, and further suggest that Irisin can act on white adipocytes

not only in an endocrine manner but also through an autocrine pathway. In addition, we further show that both antibody-mediated neutralization of Irisin in *Mstn*^{-/-} white adipocytes is able to significantly decrease the elevated expression of *ucp1* and additional BAT marker genes (*cox7a1*, *ebf3*, *hspb7* and *cidea*) observed in *Mstn*^{-/-} adipocytes when compared with control (Figure 5b). A similar reduction in *ucp1* expression was noted upon siRNA-mediated inhibition of *Fndc5* expression in *Mstn*^{-/-} adipocytes (Figures 5c and d). However, it is noteworthy to mention that antibody-mediated neutralization of Irisin was not able to completely reduce the increased *ucp1* expression in *Mstn*^{-/-} adipocytes, to the same level in WT adipocytes (Figure 5b). We therefore speculate that additional factors, other than Irisin may contribute to the enhanced browning and thermogenic gene expression observed in *Mstn*^{-/-} white adipocytes. As FGF21 signaling is also targeted by miR-34a, and given the reduced miR-34a expression in *Mstn*^{-/-} adipocytes (Figure 4b), it is likely that enhanced FGF21 signaling may also promote browning of *Mstn*^{-/-} adipocytes. However, further studies will need to be performed to assess the expression of other miR-34 targets including FGF21 receptor components in *Mstn*^{-/-} adipocytes. In addition to FGF21, we have previously shown that the loss of *Mstn* promotes the browning of WAT through a mechanism involving COX-2.¹¹ Given the fact that COX-2 can promote the expression of *ucp1* and induce browning of WAT,¹⁷ it is quite possible that enhanced COX-2 expression may also contribute to the elevated *ucp1* expression observed in *Mstn*^{-/-} adipocytes.

Mstn was initially characterized as a potent inhibitor of skeletal muscle growth and development.⁸⁻¹⁰ However, in recent years, its role in the regulation of insulin signaling, glucose and lipid metabolism has gained attention.¹¹⁻¹⁵ It is well accepted that inhibition of *Mstn* signaling improves insulin sensitivity and prevents obesity. However, there is controversy as to whether these beneficial effects are secondary to an improved metabolic phenotype in skeletal muscle, or whether *Mstn* acts as a direct regulator of glucose and lipid metabolism in other tissues. Our study strongly suggests that *Mstn* can function as a direct regulator of metabolic phenotype in tissues other than skeletal muscle. Most certainly, treatment of white adipocytes with exogenous *Mstn* resulted in the reduced expression of *Fndc5* and BAT marker genes (Figures 5e and f). Moreover, loss of *Mstn* signaling in white adipocytes promoted the development of a brown adipose tissue-like phenotype through enhancing endogenous white adipocyte *Fndc5* expression (Figures 4c and d-g). Guo *et al.*¹⁴ have shown that tissue-specific inhibition of *Mstn* signaling in skeletal muscle, rather than in adipose tissue, led to the reduced adipose tissue mass and improved insulin sensitivity. Through adipose-specific expression of dominant negative activin type IIB receptor (ActRIIB), Guo *et al.* blocked *Mstn* signaling in adipocytes and demonstrated no decrease fat mass and no metabolic benefits in mice. However, this study cannot exclude the direct role of *Mstn* in regulating adipocytes, as *Mstn* has also been shown to activate downstream signaling through binding to the activin type IIA receptor,⁴⁴ although *Mstn* binds to ActRIIB with higher affinity. Therefore, without complete blockade of *Mstn* signaling it would be difficult to rule out a direct role for *Mstn* in adipocyte metabolism.

In summary, here we have described a novel miR-34a-dependent signaling mechanism through which *Mstn* inhibits *Fndc5* expression (Figure 6). We further propose that the loss of *Mstn* results in decreased miR-34a expression, which promotes increased *Fndc5/Irisin* expression and secretion. Enhanced Irisin levels in turn drives thermogenic gene expression and the brown adipocyte-like phenotype in *Mstn*^{-/-} white adipocytes. To our knowledge, this is the first study to identify a microRNA-dependent post-transcriptional mechanism through which *Mstn* regulates metabolic function.

CONFLICT OF INTEREST

The authors declare no conflict of interest.

ACKNOWLEDGEMENTS

We thank Professor Ravi Kambadur (Nanyang Technological University) and Associate Professor Mridula Sharma (National University of Singapore) for helpful discussions. We would like to thank Professor Se-Jin Lee (The Johns Hopkins University, Baltimore, MD, USA) for gifting the *Mstn*^{-/-} mice, Dr Sabeera Bonala for preliminary studies, and Dr Prasanna Kumar Juvvuna for supply of miR-34a-overexpressing adenovirus (pacAD5-miR-34a) and control adenovirus (pacAD5-neg). We are indebted to Agency for Science, Technology and Research (A*STAR), and National Medical Research Council (NMRC), Singapore, for financial support.

REFERENCES

- 1 Cypess AM, Lehman S, Williams G, Tal I, Rodman D, Goldfine AB *et al.* Identification and importance of brown adipose tissue in adult humans. *N Engl J Med* 2009; **360**: 1509–1517.
- 2 Virtanen KA, Lidell ME, Orava J, Heglind M, Westergren R, Niemi T *et al.* Functional brown adipose tissue in healthy adults. *N Engl J Med* 2009; **360**: 1518–1525.
- 3 Saito M, Okamatsu-Ogura Y, Matsushita M, Watanabe K, Yoneshiro T, Nio-Kobayashi J *et al.* High incidence of metabolically active brown adipose tissue in healthy adult humans: effects of cold exposure and adiposity. *Diabetes* 2009; **58**: 1526–1531.
- 4 Spiegelman BM. Banting Lecture 2012: Regulation of adipogenesis: toward new therapeutics for metabolic disease. *Diabetes* 2013; **62**: 1774–1782.
- 5 Bartelt A, Heeren J. Adipose tissue browning and metabolic health. *Nat Rev Endocrinol* 2014; **10**: 24–36.
- 6 Cannon B, Nedergaard J. Brown adipose tissue: function and physiological significance. *Physiol Rev* 2004; **84**: 277–359.
- 7 Wu J, Bostrom P, Sparks LM, Ye L, Choi JH, Giang AH *et al.* Beige adipocytes are a distinct type of thermogenic fat cell in mouse and human. *Cell* 2012; **150**: 366–376.
- 8 Kambadur R, Sharma M, Smith TP, Bass JJ. Mutations in myostatin (GDF8) in double-muscled Belgian Blue and Piedmontese cattle. *Genome Res* 1997; **7**: 910–916.
- 9 Kirk S, Oldham J, Kambadur R, Sharma M, Dobbie P, Bass J. Myostatin regulation during skeletal muscle regeneration. *J Cell Physiol* 2000; **184**: 356–363.
- 10 McPherron AC, Lawler AM, Lee SJ. Regulation of skeletal muscle mass in mice by a new TGF-beta superfamily member. *Nature* 1997; **387**: 83–90.
- 11 Zhang C, McFarlane C, Lokireddy S, Masuda S, Ge X, Gluckman PD *et al.* Inhibition of myostatin protects against diet-induced obesity by enhancing fatty acid oxidation and promoting a brown adipose phenotype in mice. *Diabetologia* 2012; **55**: 183–193.
- 12 Zhang C, McFarlane C, Lokireddy S, Bonala S, Ge X, Masuda S *et al.* Myostatin-deficient mice exhibit reduced insulin resistance through activating the AMP-activated protein kinase signalling pathway. *Diabetologia* 2011; **54**: 1491–1501.
- 13 McPherron AC, Lee SJ. Suppression of body fat accumulation in myostatin-deficient mice. *J Clin Invest* 2002; **109**: 595–601.
- 14 Guo T, Jou W, Chanturiya T, Portas J, Gavrilova O, McPherron AC. Myostatin inhibition in muscle, but not adipose tissue, decreases fat mass and improves insulin sensitivity. *PLoS One* 2009; **4**: e4937.
- 15 Zhao B, Wall RJ, Yang J. Transgenic expression of myostatin propeptide prevents diet-induced obesity and insulin resistance. *Biochem Biophys Res Commun* 2005; **337**: 248–255.
- 16 Shan T, Liang X, Bi P, Kuang S. Myostatin knockout drives browning of white adipose tissue through activating the AMPK-PGC1alpha-Fndc5 pathway in muscle. *FASEB J* 2013; **27**: 1981–1989.
- 17 Madsen L, Pedersen LM, Lillefosse HH, Fjaere E, Bronstad I, Hao Q *et al.* UCP1 induction during recruitment of brown adipocytes in white adipose tissue is dependent on cyclooxygenase activity. *PLoS One* 2010; **5**: e11391.
- 18 Vegiopoulos A, Muller-Decker K, Strzoda D, Schmitt I, Chichelnitskiy E, Ostertag A *et al.* Cyclooxygenase-2 controls energy homeostasis in mice by de novo recruitment of brown adipocytes. *Science* 2010; **328**: 1158–1161.
- 19 Bostrom P, Wu J, Jedrychowski MP, Korde A, Ye L, Lo JC *et al.* A PGC1-alpha-dependent myokine that drives brown-fat-like development of white fat and thermogenesis. *Nature* 2012; **481**: 463–468.
- 20 Soukas A, Socci ND, Saatkamp BD, Novelli S, Friedman JM. Distinct transcriptional profiles of adipogenesis in vivo and in vitro. *J Biol Chem* 2001; **276**: 34167–34174.
- 21 Sharma M, Kambadur R, Matthews KG, Somers WG, Devlin GP, Conaglen JV *et al.* Myostatin, a transforming growth factor-beta superfamily member, is expressed

- in heart muscle and is upregulated in cardiomyocytes after infarct. *J Cell Physiol* 1999; **180**: 1–9.
- 22 Thomas M, Langley B, Berry C, Sharma M, Kirk S, Bass J et al. Myostatin, a negative regulator of muscle growth, functions by inhibiting myoblast proliferation. *J Biol Chem* 2000; **275**: 40235–40243.
- 23 McFarlane C, Vajjala A, Arigela H, Lokireddy S, Ge X, Bonala S et al. Negative auto-regulation of myostatin expression is mediated by Smad3 and microRNA-27. *PLoS One* 2014; **9**: e87687.
- 24 Ge X, McFarlane C, Vajjala A, Lokireddy S, Ng ZH, Tan CK et al. Smad3 signaling is required for satellite cell function and myogenic differentiation of myoblasts. *Cell Res* 2011; **21**: 1591–1604.
- 25 Picard V, Ersdal-Badju E, Lu A, Bock SC. A rapid and efficient one-tube PCR-based mutagenesis technique using Pfu DNA polymerase. *Nucleic Acids Res* 1994; **22**: 2587–2591.
- 26 Lokireddy S, Wijesoma IW, Teng S, Bonala S, Gluckman PD, McFarlane C et al. The ubiquitin ligase Mul1 induces mitophagy in skeletal muscle in response to muscle-wasting stimuli. *Cell Metab* 2012; **16**: 613–624.
- 27 Lee P, Werner CD, Kebebew E, Celi FS. Functional thermogenic beige adipogenesis is inducible in human neck fat. *Int J Obes (Lond)* 2014; **38**: 170–176.
- 28 Huh JY, Panagiotou G, Mougios V, Brinkoetter M, Vamvini MT, Schneider BE et al. FND5 and irisin in humans: I. Predictors of circulating concentrations in serum and plasma and II. mRNA expression and circulating concentrations in response to weight loss and exercise. *Metabolism* 2012; **61**: 1725–1738.
- 29 Roca-Rivada A, Castelao C, Senin LL, Landrove MO, Baltar J, Belen Crujeiras A et al. FND5/irisin is not only a myokine but also an adipokine. *PLoS One* 2013; **8**: e60563.
- 30 Jedrychowski MP, Wrann CD, Paulo JA, Gerber KK, Szpyt J, Robinson MM et al. Detection and Quantitation of Circulating Human Irisin by Tandem Mass Spectrometry. *Cell Metab* 2015; **22**: 734–740.
- 31 McPherron AC, Lee SJ. Double muscling in cattle due to mutations in the myostatin gene. *Proc Natl Acad Sci USA* 1997; **94**: 12457–12461.
- 32 Hittel DS, Berggren JR, Shearer J, Boyle K, Houmard JA. Increased secretion and expression of myostatin in skeletal muscle from extremely obese women. *Diabetes* 2009; **58**: 30–38.
- 33 Milan G, Dalla Nora E, Pilon C, Pagano C, Granzotto M, Manco M et al. Changes in muscle myostatin expression in obese subjects after weight loss. *J Clin Endocrinol Metab* 2004; **89**: 2724–2727.
- 34 Ortega FJ, Moreno-Navarrete JM, Pardo G, Sabater M, Hummel M, Ferrer A et al. MiRNA expression profile of human subcutaneous adipose and during adipocyte differentiation. *PLoS One* 2010; **5**: e9022.
- 35 Yan B, Shi X, Zhang H, Pan L, Ma Z, Liu S et al. Association of serum irisin with metabolic syndrome in obese Chinese adults. *PLoS One* 2014; **9**: e94235.
- 36 Zhang HJ, Zhang XF, Ma ZM, Pan LL, Chen Z, Han HW et al. Irisin is inversely associated with intrahepatic triglyceride contents in obese adults. *J Hepatol* 2013; **59**: 557–562.
- 37 Choi YK, Kim MK, Bae KH, Seo HA, Jeong JY, Lee WK et al. Serum irisin levels in new-onset type 2 diabetes. *Diabetes Res Clin Pract* 2013; **100**: 96–101.
- 38 Moreno-Navarrete JM, Ortega F, Serrano M, Guerra E, Pardo G, Tinahones F et al. Irisin is expressed and produced by human muscle and adipose tissue in association with obesity and insulin resistance. *J Clin Endocrinol Metab* 2013; **98**: E769–E778.
- 39 Liu JJ, Wong MD, Toy WC, Tan CS, Liu S, Ng XW et al. Lower circulating irisin is associated with type 2 diabetes mellitus. *J Diabetes Complications* 2013; **27**: 365–369.
- 40 Fu T, Seok S, Choi S, Huang Z, Suino-Powell K, Xu HE et al. MiR-34a inhibits beige and brown fat formation in obesity in part by suppressing adipocyte FGF21 signaling and SIRT1 function. *Mol Cell Biol* 2014; **34**: 4130–41342.
- 41 Fu T, Choi SE, Kim DH, Seok S, Suino-Powell KM, Xu HE et al. Aberrantly elevated microRNA-34a in obesity attenuates hepatic responses to FGF19 by targeting a membrane coreceptor beta-Klotho. *Proc Natl Acad Sci USA* 2012; **109**: 16137–16142.
- 42 Fisher FM, Kleiner S, Douris N, Fox EC, Mepani RJ, Verdeguer F et al. FGF21 regulates PGC-1alpha and browning of white adipose tissues in adaptive thermogenesis. *Genes Dev* 2012; **26**: 271–281.
- 43 Kharitonov A, Adams AC. Inventing new medicines: the FGF21 story. *Mol Metab* 2014; **3**: 221–229.
- 44 Tsuchida K, Nakatani M, Uezumi A, Murakami T, Cui X. Signal transduction pathway through activin receptors as a therapeutic target of musculoskeletal diseases and cancer. *Endocr J* 2008; **55**: 11–21.



This work is licensed under a Creative Commons Attribution-NonCommercial-NoDerivs 4.0 International License. The images or other third party material in this article are included in the article's Creative Commons license, unless indicated otherwise in the credit line; if the material is not included under the Creative Commons license, users will need to obtain permission from the license holder to reproduce the material. To view a copy of this license, visit <http://creativecommons.org/licenses/by-nc-nd/4.0/>

© The Author(s) 2017

Supplementary Information accompanies this paper on International Journal of Obesity website (<http://www.nature.com/ijo>)